

Transient Formulations for a Heat-Generating Fin with a Temperature-Dependent Heat Transfer Coefficient and Thermal Conductivity

Okey Oseloka Onyejekwe

Computational Science Program, Addis Ababa University, Arat Kilo Campus, Addis Ababa Ethiopia

*Corresponding author

Okey Oseloka Onyejekwe, Computational Science Program, Addis Ababa University, Arat Kilo Campus, Addis Ababa Ethiopia; E-Mail: okuzaks@yahoo.com

Submitted: 27 Mar 2019; Accepted: 08 Apr 2019; Published: 29 May 2019

Abstract

Numerical calculations and scalar transport analyses are carried out for transient heat transfer in a heat generating fin with a temperature-dependent heat transfer and conduction coefficients. The highly nonlinear governing equation, satisfies the Dirichlet and Neumann boundary conditions at both ends of the problem domain. Integral representation of the governing equation over the discretized problem domain is achieved via the Green's second identity together with the so called free-space Green function. This element-driven approach together with the finite difference approximation of the temporal derivative result in discrete equations which are recursive in nature. At the boundaries of any of the adjacent elements, compatibility conditions and/or boundary conditions are enforced to guarantee scalar continuity. After the resulting system of discrete equations are numerically solved and assembled, they yield the transient history of the scalar variables at any particular point in time. Several numerical tests are carried out to ensure the convergence and accuracy of the formulation by comparing numerical results with those found in literature.

Keywords: Nonlinear Differential Equation, Free- Space Green Function, Fundamental Solution, Transient Heat Transfer, Temperature Dependent Heat Transfer and Conduction Coefficients, Integral Representation, Elements, Complementary Differential Equation, Compatibility Conditions.

Introduction

The nonlinear governing equation representing heat transfer through extended surfaces illustrates conservation of energy. Its complex characteristics defy tidy analytical solutions and as such it is only amenable to approximate analytical or numerical solutions. These include Taylor transformation methods [1-3], Adomian decomposition methods and power series methods [4-7]. Other methods based on spatial/temporal discrete techniques comprise finite element/finite difference methods [8, 9]. Very few exact solutions exist for the one-dimensional fin problem. These are only possible for constant heat transfer coefficient and thermal conductivity. However with some considerable effort Moitsheki et al. were able to arrive at exact solutions for a fin problem with a given nonlinear thermal conductivity and heat transfer coefficient. In a later work, Mhlongo and Moitsheki [10, 11], extended the analysis to account for temperature distributions for fins of different profiles. Although a good number of works on fins is based on steady state analysis, there exist situations where knowledge of transient response is necessary. This is true of fans incorporating moving fins, electronic cooling components, heat exchanger nuclear reactors etc.

One of the earliest works on fins involving transient computation was carried out by Chapman [12]. He developed equations that yielded information for transient temperature response of fins for cases involving dissipation of heat to the surroundings and the relationship between temperature distribution and base heat. Donaldson and Shouman later developed equations for fin transient temperature distribution for two cases involving step changes in base heat flow rate and base temperature distribution [13]. We hasten to comment that most of the work done on fins at this stage, relied heavily on analytical and graphical techniques. Very much along these lines are contributions from Aziz and Kraus who adopted a separation of variables approach to determine temperature profiles for a convecting straight fin with a step change and Suryanarayana who solved a similar problem but instead of using the same approach adopted by employed the Laplace transform technique [14, 15]. The Laplace transform method was also applied by Mao and Rooke to investigate temperature profiles involving step changes for different fin configurations [16].

However a slightly different picture arises for real world situations encountered in engineering practice namely for the case of (i) a solid protrusion with temperature dependent thermal conductivity and/or variable specific heat exposed to an ambient fluid and attached to a heat source and whose transient temperature profile is dictated by physically realistic boundary conditions (ii) a solid protrusion with nonlinear thermo-physical properties and subjected to internal heat generation. Application of the above mentioned techniques

for this class of problems comes with certain limitations especially those that arise from nonlinearities and certain boundary condition specifications. It therefore comes as a little or no surprise that in the majority of such cases recourse has to be made to numerical techniques.

Mosayebidorcheh et al. implemented a transient thermal analysis of longitudinal fins with internal heat generation and nonlinear temperature dependent properties. They adopted a hybrid numerical technique based on differential transform method (DTM) and finite difference method (FDM) to study the effects of such fin parameters as thermal conductivity, shape profile, convection heat transfer coefficient and internal heat generation on the overall temperature distribution. In another related work, Onur, Aziz and Torabi carried out a transient numerical analysis of heat transfer characteristics of a fin with temperature dependent heat transfer coefficient. One of the earliest contributions to the numerical study of fins with circular geometry was made by Campo [17-20]. He considered a circular fin with coupled convection and radiation heat transfer. He analyzed the problem setup for two cases namely, for the first type, the fin at ambient temperature was exposed to a harmonic oscillation at its base for zero time while for the second, and the fin was exposed to a non-uniform temperature initially except at the base, where the temperature variation is periodic. The resulting governing partial differential equation was finally reduced to a system of first order ordinary differential equations and solved numerically to yield the temperature field and the accompanying heat flux. Later work on transient numerical computations for fins considered different geometries. Moitsheki and Harley worked on transient heat transfer in longitudinal fins of various profiles with temperature dependent thermal conductivity and heat transfer coefficient [21]. They originally applied a classical Lie point symmetry approach involving some reductions in the governing differential equations. However they found out that for certain interesting cases, the initial and boundary conditions were not invariant under the admitted Lie point symmetries and the governing differential equation was therefore solved numerically to handle this challenge. This was a sequel to the work earlier done by Moitsheki whereby he applied some rudiments of Lie group techniques to an unsteady nonlinear diffusion problem to model thermal energy storage in a medium with temperature-dependent power law thermal conductivity [22].

Further work on transient temperature distribution was carried out by Campo in his study of heat transfer in a convecting slab with variable thermo-physical properties. He solved the resulting energy equation directly by reducing it to a pair of related equations via transformation schemes in order to alleviate the inherent nonlinearities. Campo and Salazar also employed a computational scheme known as the Transversal Method of Lines (TMOL) to explore the relationship between transient conduction in a planar slab for a short period of time and the steady state conduction of a straight fin of uniform cross-section [23, 24]. The result of their study was very useful for providing short-time scalar distributions for a fin subjected to Dirichlet or Robin-type boundary conditions for which the heat transfer coefficient is very large and the nonlinear heat conduction relatively small. Malekzadeh et al. applied the differential quadrature method (DQEM) to solve a fin problem involving nonlinear boundary conditions. This method, involved a finite element method (FEM)-type domain and temporal discretization with no restrictions for time steps and grid spacing [25]. Their results provided accurate solutions for fin problems involving convective-radiative heat

transfer conditions. Convergence, stability and reliability of the scheme were confirmed for various test cases involving complex geometries for various levels of nonlinearity.

Sobamowo produced one of the few attempts involving the use of numerical integral techniques for fin study. He used the Galerkin method of weighted residual to analyze the effects of thermo-geometric parameters, coefficient of heat transfer, and nonlinear thermal conductivity parameters on the temperature field. His numerical effort not only showed the dependence of the scalar field on the fin's thermo-geometric properties but in addition determined the limiting values of the fin's parameters outside of which the fin can no longer operate optimally. The same numerical approach was adopted by Sobamowo et al. to study the thermal performance of a natural convection porous fin with temperature-dependent thermal conductivity and internal heat generation [26, 27].

The preceding literature review has brought into focus the preponderance of approximate analytic techniques for the solution of the nonlinear fin problem and the paucity of integro-numerical techniques especially of the boundary element variety to accomplish the same task. The reason is not far-fetched. Boundary element method (BEM)-based techniques automatically loses one of its most cherished advantage i.e. dimensionality-reduction if applied to a one-dimensional problem no matter how challenging the problem is. Instead the route to one-dimensional application is through a similar two-dimensional problem accompanied by an application of the no-flux condition at the top and bottom boundaries [28-30]. Apart from introducing unnecessary complications into the problem formulation often times the physics of the problem is compromised.

The work reported herein adopts a completely different approach and aims at a straightforward way of solving a relatively complicated problem by providing a comprehensive numerical method for resolving a nonlinear transient heat transfer process in a fin accompanied by internal heat generation. A hybrid domain-discretized numerical procedure is applied in the spatial domain, while classical methods such as the finite difference are used to resolve the time dimension. Flexibility of this approach permits the variation of the thermal parameters in both space and time. The problem domain is discretized into elements, and their corresponding equations are derived while the boundary conditions as well as the compatibility conditions at the interface of the elements are enforced. This is followed by a finite-element-type assembly of the element equations and eventual solution to yield the scalar variables at the nodes of each element. Convergence and accuracy of the numerical results are confirmed by a series of test cases with various levels of rigor and loading. Details of the development of this technique and its application can be found in Onyejekwe [27].

Problem Formulation

We consider a longitudinal one-dimensional fin described by a constant cross-sectional area A_c , a temperature-dependent thermal conductivity $k(T)$ and heat transfer coefficient $h(T)$, thickness δ , and length L . The spatial and the temporal coordinates are given by x and t respectively. The perimeter of the fin is denoted by P and it is attached to a fixed body of temperature T_b . It extends into a fluid of ambient temperature T_∞ . In addition there exists a temperature-dependent heat generation per unit volume within the fin specified by $Q(T)$. The non-linear, transient one-dimensional heat balance equation in dimensional form can be written as

$$\rho c \frac{\partial T}{\partial t} = \frac{\partial}{\partial x} \left[k(T) \frac{\partial T}{\partial x} \right] - \frac{h(T)}{A_c} P(T - T_\infty) + q(T) \quad (1)$$

Both the thermal conductivity and internal heat generation terms in many engineering applications are assumed to be linear functions of temperature and are given as

$$K = k_\infty [1 + \lambda(T - T_\infty)] \quad (2)$$

where k_∞ is the thermal conductivity of the fin at ambient temperature and λ is a parameter that controls the dependence of conductivity on temperature.

$$q(T) = q_\infty [1 + \phi(T - T_\infty)] \quad (2b)$$

where ϕ is the internal heat generation gradient? The heat transfer coefficient is expressed by a power law used in many industrial applications [21]

$$h(T) = h_b \left(\frac{T - T_\infty}{T_b - T_\infty} \right)^n \quad (2c)$$

where h_b is the heat transfer coefficient at the base temperature? The exponent n depends on the heat transfer mode and usually varies between -6.6 and 5. However for most practical applications it has been found to lie in the neighborhood of -3 and 3 [21]. With the introduction of the following dimensionless variables

$$\begin{aligned} \chi &= \frac{x}{L}, \quad \theta = \frac{T - T_\infty}{T_b - T_\infty}, \quad \tau = \frac{k_a t}{\rho c L^2}, \quad h = \frac{H}{h_b} \\ k &= \frac{K}{k_a}, \quad \psi^2 = \frac{P h_b L^2}{A_c k_a}, \quad Q = \frac{q_a A_c}{h_b P (T_b - T_\infty)} \\ \gamma &= \phi (T_b - T_\infty), \quad \beta = \lambda (T_b - T_\infty) \end{aligned} \quad (3)$$

Equation (1) reduces to a dimensionless energy equation expressed as

$$\frac{\partial \theta}{\partial \tau} = \frac{\partial}{\partial X} \left[(1 + \beta \theta) \frac{\partial \theta}{\partial X} \right] - \psi^2 \theta^{(n+1)} + \psi^2 Q (1 + \gamma \theta) \quad (4)$$

An insulated fin tip with the other end at a base temperature, represent Dirichlet and Neumann type boundary conditions given as:

$$\theta(t, 0) = 1 \quad \left. \frac{\partial \theta}{\partial X} \right|_{x=L} = 0 \quad (5a)$$

Initially the fin is kept at an initial temperature

$$\theta(0, X) = 0 \quad (5b)$$

Solution Procedure

The numerical formulation adopted herein is based on the Fredholm singular integral theory which employs the free-space Green's function of the Laplace's differential operator. This application has earlier been utilized in previous work and as such is not described in detail. Equation (4) is recast to read:

$$\frac{\partial^2 \theta}{\partial \chi^2} = \left[-\frac{\partial \ln D(\theta)}{\partial X} \frac{\partial \theta}{\partial \chi} + \frac{1}{D(\theta)} \left\{ \psi^2 (\theta^{(n+1)} + (1 + \gamma \theta)) + \frac{\partial \theta}{\partial \tau} \right\} \right] \quad (6)$$

where $D(\theta) = 1 + \beta \theta$. Applying the Green's second identity to equation (6) yields

$$\begin{aligned} & \left[-\zeta \theta(X_i, \tau) + G^*(\chi_2, \chi_i) \theta(X_2, \tau) - G^*(\chi_1, \chi_i) \theta(X_1, \tau) \right. \\ & \quad \left. - G(\chi_2, \chi_i) \varphi(X_2, \tau) + G(\chi_1, \chi_i) \varphi(X_1, \tau) \right] \\ & \quad \int_{\chi_1}^{\chi_2} G(\chi, \chi_i) \left(\frac{\partial^2 \theta}{\partial \chi^2} \right) d\chi = 0; \quad i = 1, 2 \end{aligned} \quad (7)$$

where $G(\chi, \chi_i) = (|\chi - \chi_i| + \Phi)/2$ is the free-space Green's function and Φ is an arbitrary function which is set equal to the longest element in the computational domain, φ , is the spatial derivative of the dependent variable or the 'flux', ζ is a parameter that is set to unity when the source node χ_i is within the element or 0.5 when it is at the nodes of an element, and $G^* = dG(\chi, \chi_i)/d\chi$. Next, in order to facilitate the computation of the line integral, we approximate all the functional quantities that constitute the kernel with linear shape functions. For example

$$-\frac{1}{D(\theta)} \frac{\partial D(\theta)}{\partial \chi} \frac{\partial \theta}{\partial \chi} = -\Omega_m \kappa_m \left(\frac{1}{l} \frac{d\Omega_n}{d\xi} D_n \right) \Omega_j \varphi_j \quad (8)$$

where the element shape functions are defined as $\Omega_1 = (\chi_2 - \chi)/l$, $\Omega_2 = (\chi - \chi_1)/l$. In order to enhance elemental integration, it is convenient to convert to a local coordinate system that takes χ_1 as the origin. This is expressed as $\xi = (\chi - \chi_1)/l$, as a consequence, $\Omega_1 = (1 - \xi)$, $\Omega_2 = \xi$. Substituting the expressions for the free-space Green's function, as well as the interpolation approximations into equation (7) yields the matrix equation

$$R_{ij} \theta_j + (L_{ij} - \Theta_{imnj} D_m \Lambda_n) \varphi_j + M_{ijm} \Lambda_m \left(\frac{d\theta_j}{dt} + F_j \right) = 0, \quad i, j, m, n = 1, 2 \quad (9)$$

The transient term is discretized by a two-level time discretization scheme and is substituted into equation (9) to yield

$$\begin{aligned} & \left[\alpha R_{ij} + M_{inj} \left\{ \frac{\alpha \Lambda_n^{(m+1)} + (1 - \alpha) \Lambda_n^{(m)}}{\Delta \tau} \right\} \right] \theta_j^{(m+1)} + \alpha [L_{ij} - \Theta_{imnj} D_m^{(m+1)} \Lambda_n^{(m+1)}] \varphi_j^{(m+1)} + \\ & \left[(1 - \alpha) R_{ij} + M_{inj} \left\{ \frac{\alpha \Lambda_n^{(m+1)} + (1 - \alpha) \Lambda_n^{(m)}}{\Delta \tau} \right\} \right] \theta_j^{(m)} + (1 - \alpha) [L_{ij} - \Theta_{imnj} D_m^{(m+1)} \Lambda_n^{(m+1)}] \varphi_j^{(m)} + \\ & M_{inj} [\alpha \Lambda_n^{(m+1)} + (1 - \alpha) \Lambda_n^{(m)}] [\alpha F_n^{(m+1)} + (1 - \alpha) F_n^{(m)}] = 0 \quad i, j, m, n = 1, 2, \quad 0 \leq \alpha \leq 1 \end{aligned} \quad (10)$$

Equation (10) is a system of nonlinear equations solved for each element in a discretized problem domain. We choose the Picard algorithm to handle the nonlinearity in this case, and equation (10) is recast to read:

$$\left\{ \begin{aligned} & \left[\alpha R_y + M_{iy} \left\{ \frac{\alpha \Lambda_n^{(m+1)} + (1-\alpha) \Lambda_n^{(m)}}{\Delta \tau} \right\} \right] \theta_j^{(m+1,s+1)} + \alpha [L_y - \Theta_{my} D_m^{(m+1,s)} \Lambda_n^{(m+1,s)}] \phi_j^{(m+1,s+1)} = \\ & - \left[(1-\alpha) R_y + M_{iy} \left\{ \frac{\alpha \Lambda_n^{(m+1)} + (1-\alpha) \Lambda_n^{(m)}}{\Delta \tau} \right\} \right] \theta_j^{(m,s)} + (1-\alpha) [L_y - \Theta_{my} D_m^{(m+1,s)} \Lambda_n^{(m+1,s)}] \phi_j^{(m,s)} + \\ & M_{iy} [\alpha \Lambda_n^{(m+1)} + (1-\alpha) \Lambda_n^{(m)}] [\alpha F_n^{(m+1)} + (1-\alpha) F_n^{(m)}] \end{aligned} \right\} \quad (11)$$

$i, j, m, n = 1, 2, \quad 0 \leq \alpha \leq 1$

where s and $s+1$ denote the current and previous iteration levels. Equation (11) is a hybrid BEM-FEM discretization of the nonlinear fin problem together with heat generation and nonlinear conduction and heat transfer coefficient parameters. As each elemental equation is nonlinear, the Picard iterative procedure is implemented at each time step until convergence is achieved. Since the integral element equation is solved for each element of the discretized problem domain, the coefficient matrix is banded and its entries are dependent on the solution at previous iteration.

The code developed herein obtains solutions (the dependent variable and its spatial coordinate) at different time steps by adopting linear approximations for the dependent variables as well as linear finite difference time approximation. The resulting matrix equation is of the type:

$$[A]_{i,j}^{(m+1,s)} \begin{Bmatrix} \theta \\ \phi \end{Bmatrix}_j^{(m+1,s+1)} = \mathfrak{F}_j^{(m+1,s)} \quad (12)$$

Results and Discussions

The validity of the algorithm developed herein was tested by comparing the numerical results with those obtained from analytic and finite element solutions as shown in Table 1. The fin parameters are the same as those found in [26]. The magnitude of the relative errors demonstrates that this numerical technique is closer to the analytic than FEM and can be relied on for other challenging computations.

Table 1: Numerical Vs. Analytic Solution

| Grid Points | Current Work | Analytic Results | FEM results (Ref. 26) | Relative Errors Current Work | Relative Errors (FEM Results) |
|--------------|--------------|------------------|-----------------------|------------------------------|-------------------------------|
| 0000000E+00 | 0.7888016 | 0.7888326 | 0.7857143 | 3.9367060E-05 | 3.9292681E-03 |
| 5.000001E-02 | 0.7892877 | 0.7893187 | 0.7862500 | 3.9191789E-05 | 3.8635940E-03 |
| 0.1000000 | 0.7907478 | 0.7907783 | 0.7878571 | 3.8591825E-05 | 3.6690740E-03 |
| 0.1500000 | 0.7931847 | 0.7932152 | 0.7905357 | 3.8398124E-05 | 3.3509040E-03 |
| 0.2000000 | 0.7966052 | 0.7966352 | 0.7942857 | 3.7634716E-05 | 2.9201773E-03 |
| 0.2500000 | 0.8010176 | 0.8010470 | 0.7991071 | 3.6757760E-05 | 2.3907283E-03 |
| 0.3000000 | 0.8064328 | 0.8064617 | 0.8050000 | 3.5771878E-05 | 1.7799205E-03 |
| 0.3500000 | 0.8128647 | 0.8128927 | 0.8119643 | 3.4389013E-05 | 1.1089741E-03 |
| 0.4000000 | 0.8203292 | 0.8203561 | 0.8200000 | 3.2840981E-05 | 4.0145908E-04 |
| 0.4500000 | 0.8288446 | 0.8288707 | 0.8291072 | 3.1496871E-05 | 3.1667613E-04 |
| 0.5000001 | 0.8384330 | 0.8384577 | 0.8392857 | 2.9501700E-05 | 1.0160588E-03 |
| 0.5500001 | 0.8491219 | 0.8491411 | 0.8505358 | 2.2602482E-05 | 1.6623426E-03 |
| 0.6000001 | 0.8609224 | 0.8609475 | 0.8628572 | 2.9146442E-05 | 2.2422792E-03 |
| 0.6500001 | 0.8738659 | 0.8739066 | 0.8762500 | 4.6515692E-05 | 2.7208286E-03 |
| 0.7000001 | 0.8881473 | 0.8880506 | 0.8907143 | 1.0886624E-04 | 2.8819491E-03 |
| 0.7500001 | 0.9030958 | 0.9034150 | 0.9062501 | 3.5337301E-04 | 3.4805823E-03 |
| 0.8000001 | 0.9205891 | 0.9200383 | 0.9228572 | 5.9874263E-04 | 2.4576029E-03 |
| 0.8500001 | 0.9371783 | 0.9379619 | 0.9405358 | 8.3545217E-04 | 3.5698053E-03 |
| 0.9000002 | 0.9580032 | 0.9572307 | 0.9592858 | 8.0705289E-04 | 1.3370080E-03 |
| 0.9500002 | 0.9773933 | 0.9778929 | 0.9791072 | 5.1090069E-04 | 1.7505045E-03 |
| 1.000000 | 1.000000 | 1.000000 | 1.000000 | 0.0000000E+00 | 0.0000000E+00 |

Effect of power law index

Equation (4) shows the fin parameters that influence the transient response of fins to heat dissipation and energy transport. They are the conduction parameter β , the power law exponent n , heat generation parameter Q , the heat generation coefficient γ and the thermo-geometric parameter ψ . The heat energy entering at $X=0$ comprises conduction heat transfer as well as the energy due to convection. The instantaneous base heat flow can be represented in dimensionless form as $Q_b = \partial\theta/\partial X(1, \tau)$. The instantaneous rate of energy storage in the fin can be derived from energy conservation principles as: $Q_{\text{stored}} = Q_{\text{gen}} + Q_b - Q_{\text{loss}}$; where Q_{gen} is the heat generation term supplied to the fin and Q_{loss} is the instantaneous heat loss is essentially due to convection from the fin Q_{loss} . It must be noted that when

radiation effects are not considered this is the primary source of heat loss. In order for the analysis not to become unwieldy, the transient response of each of these parameters is computed for the heat energy and temperature fields. Figure 1a shows the effect of the power law exponent on the transient dimensionless temperature field for the following values of fin parameters; $n=1.0$, $\beta=1.0$, $\psi=1.0$, $Q=0.0$, $\gamma=0.1$. The steepest profile is displayed at a dimensionless time $\tau=0.1$. As time progresses however the profile becomes flatter as the magnitude of the temperature increases. It can be surmised that as time progresses and we approach steady state performance, the temperature field will become time- invariant and run parallel to the time axis. This trend may be compared at least qualitatively with the Sobamowo who conducted studies on steady-state heat conduction

in a fin using the Galerkin method approach [26]. Figure 1b shows the dimensionless temperature field run with the same values of fin parameters, but with the power law index increased ($n=2$). The profiles show higher fin temperatures with a higher value for the n parameter with no internal heat generation. The whole effect is more pronounced at the tip of the fin. Fig. 1c shows the effect of the power law exponent n on the base heat flux, Q_b heat storage Q_s and total heat flux Q_f for the following fin parameters:

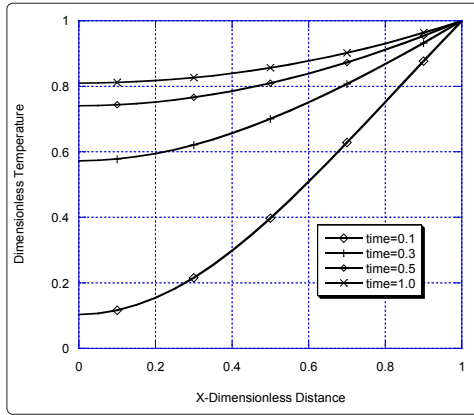


Figure 1a: Effect of power law exponent $n=1$ on dimensionless temperature

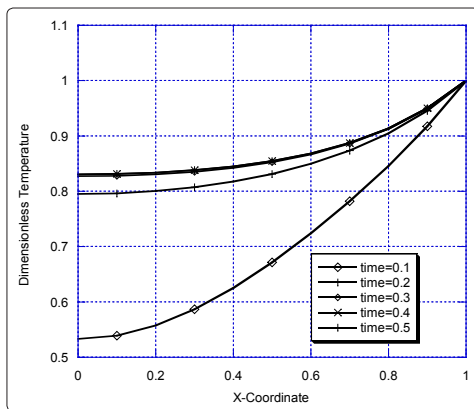


Figure 1b: Effect of power law exponent $n=2$ on dimensionless temperature

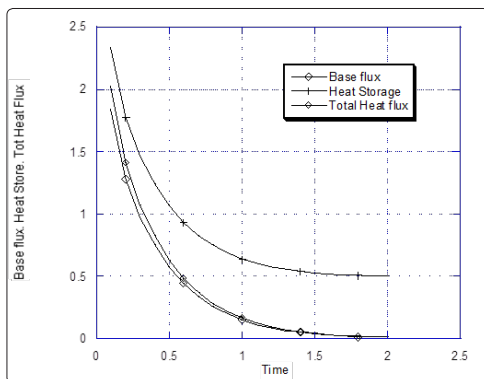


Figure 1c: Effect of power law exponent $n=1$ on heat profile

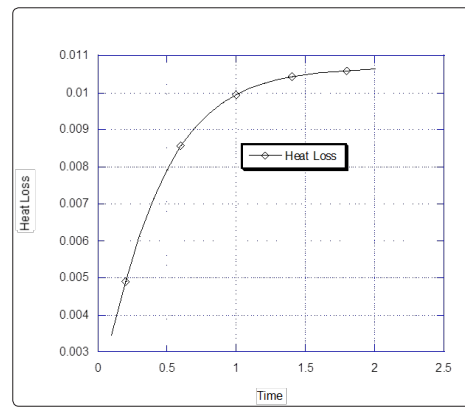


Figure 1d: Effect of power law exponent $n=1$ on heat loss

$\beta=0.1$, $n=1.0$, $\psi=0.1$, $Q=0.5$, $\gamma=0.4$ while Fig 1d shows the accompanying heat loss term for the same value of fin parameters. From Fig. 1d, it can be seen that at the very early part of the transient process, the heat loss rises gradually almost imperceptibly because great percentage of the energy in the fin from the base of the fin and the heat generation component are still stored in the fin. This can be seen from Fig. 1c where the heat storage component has the highest magnitude. Fig. 1d shows that as time progresses, the surface heat loss increases and the stored energy, total heat flux and base flux components decrease as well. We observe that when the fin achieves steady state operation approximately at $\tau \approx 1.5$, the heat storage term approaches a value of 0.5 asymptotically which is the value of the heat generation term while both the base and the total heat flux tend to a zero value while the heat storage term approach Q_{gen} asymptotically.

Effect of thermo-geometric parameter

The effect of changes in the profiles of both the dimensionless fin temperature and heat profiles are determined for the following fin parameters $Q_{gen}=0.5$, $\beta=1.0$, $n=1.0$, $\gamma=0.1$. Figures 2a ($\psi=1.0$) and 2b ($\psi=2.5$) show that the dimensionless fin profile at each node is higher the fin thermos-geometric parameter operates at a lower value. The magnitude of the difference is found to increase as time progresses. Since this parameter relates to convection of heat out of the fin; it is clear that the higher the more the heat is withdrawn from the system for a lower value of ψ and the temperature profile becomes higher. Figure 2c ($\psi=1.0$) as well as Figure 2d ($\psi=2.0$) show the instantaneous base heat flow, heat gain, heat loss and heat store respectively. The base heat flow as well as the surface heat loss is remarkably enhanced eventhough they retain similar shapes. For both cases, as time progresses the base heat flow and the surface heat loss do not become equal instead the difference between them is accounted for by the approximate magnitude of the heat generated in the fin Q_{gen} for the case of $\psi=1.0$ and almost twice as much for the higher value of thermos-geometric parameter. There is a considerable loss of heat for $\psi=2$. It happens to such an extent that fin becomes dysfunctional at $\tau \approx 0.5$, but on the contrary starts gaining heat as illustrated by the negative sign of the heat loss energy component.

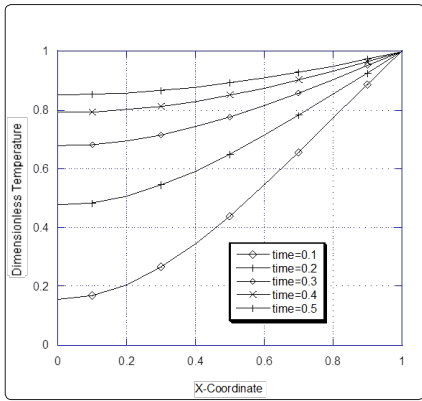


Figure 2a: Effect of thermo-geometric parameter $\xi=1$ on dimensionless temperature

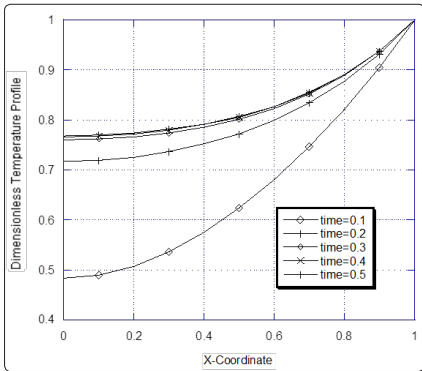


Figure 2b: Effect of thermo-geometric parameter $\xi=3$ on dimensionless temperature

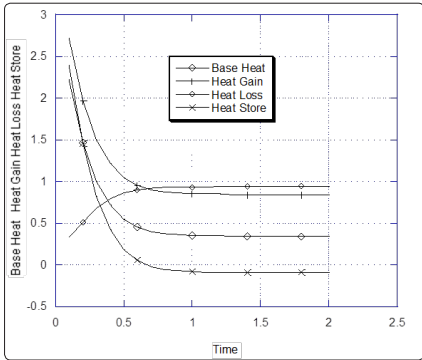


Figure 2c: Effect of thermo-geometric parameter $\xi=1$ on heat profile

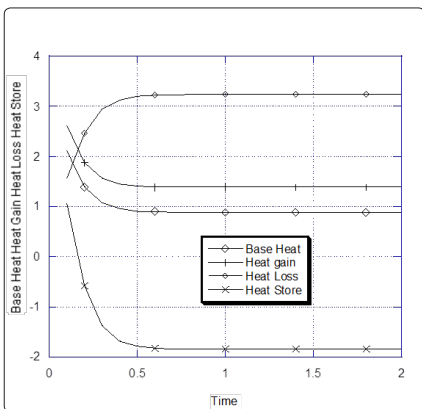


Figure 2d: Effect of thermo-geometric parameter $\xi=3$ on heat profile

Effect of internal heat generation

The effect of the internal heat generation are illustrated for the following fin parameters: $\beta=1.0$, $n=1.0$, $\psi=1.0$, $\gamma=0.1$. Figures 3a and 3b illustrate cases for no heat generation ($Q_{gen}=0.0$) and heat generation ($Q_{gen}=3.0$). As expected the higher value of the heat generation parameter displays higher temperatures profile as compared with those where there is no internal heat generation. The maximum difference is accomplished at steady state. In addition as time progresses the no heat generation profiles become less steep as steady state is approached. On the contrary the other profiles display a considerable slope reversal after $\tau \geq 0.2$. The reason for this is obvious. At this time, the fin is no longer able to remove heat from its primary surface and the fin configuration can be termed as dysfunctional. Values of the fin parameters as well as the time at which this occurs, can be considered as valuable design parameters. Figures 3c and 3d show the heat profiles for these two cases. Figure 3d shows that the heat loss term Q_{loss} is higher than that of figure 3c due to the higher temperature generation. All the other heat components decrease asymptotically until steady state is reached at $\tau \geq 0.57$. With the profiles of Fig. 3d showing more rapid decline than those of Fig. 3c where there is no heat generation.

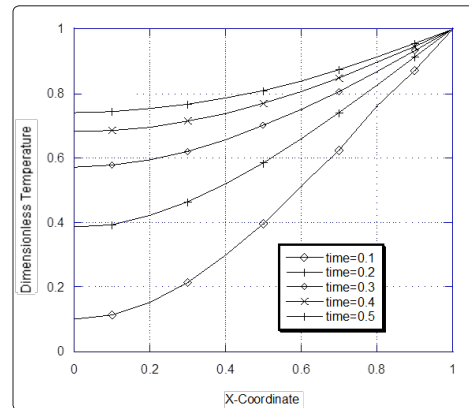


Figure 3a: Effect of conduction parameter $\beta=0.0$ on dimensionless temperature

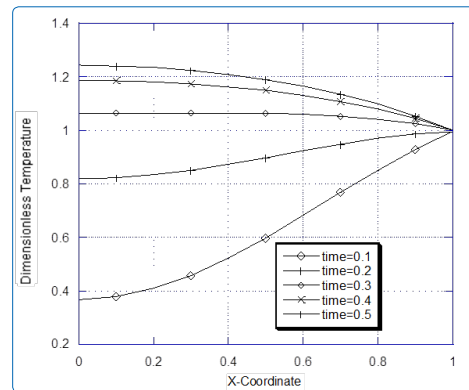


Figure 3b: Effect of conduction parameter $\beta=3.0$ on dimensionless temperature

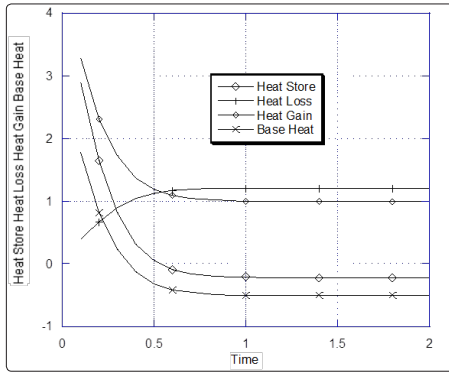


Figure 3c: Effect of conduction parameter $\beta=0.0$ on heat profile

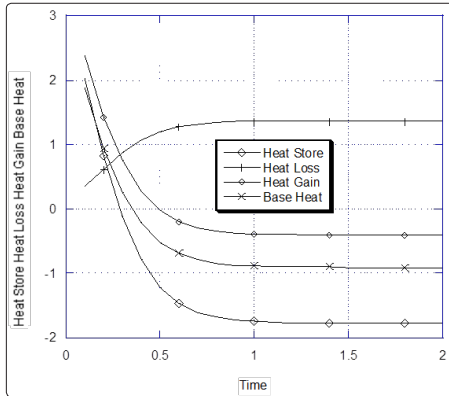


Figure 3d: Effect of conduction parameter $\beta=3.0$ on heat profile

Effect of conduction parameter

The conduction parameter is varied for the following fin parameter values $\psi=1.0$, $Q_{gen}=0.5$, $\gamma=0.1$. Figures 4a and 4b display the temperature profiles for $\beta=0.0$ and $\beta=3.0$ respectively. Higher temperature profiles are displayed for the latter case as the profiles approach steady state with a flatter temperature profile. The heat profiles if Fig. 4a reflects the temperature profile in Fig. 4a where it takes a much longer time to achieve steady state. In addition Fig.4c shows that there is a continuous loss of heat by convection until $\tau \geq 1.0$. This is unlike Fig. 4d where steady state comes much earlier ($\tau \leq 0.5$). Heat loss is mostly by convection as exemplified by the value of the thermo-geometric parameter ($\psi=1.0$). Fig. 4d displays the heat loss term rising asymptotically to a value of 1.0 and in addition, the increase in the increase in the base temperature gradient is reflected by an increase in the base heat flow.

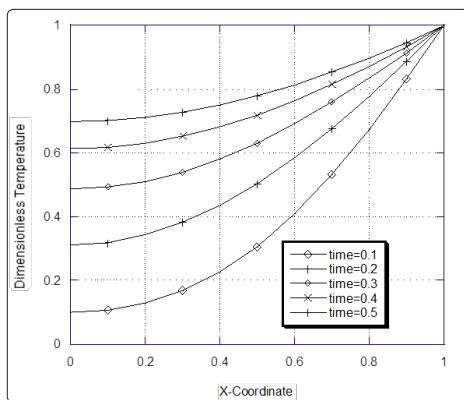


Figure 4a: Effect of heat generation parameter $Q_{gen}=1$ on dimensionless temperature

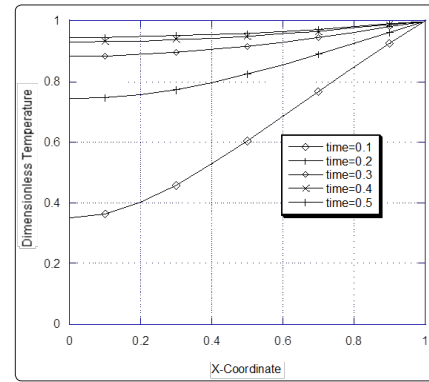


Figure 4b: Effect of heat generation parameter $Q_{gen}=2.5$ on dimensionless temperature

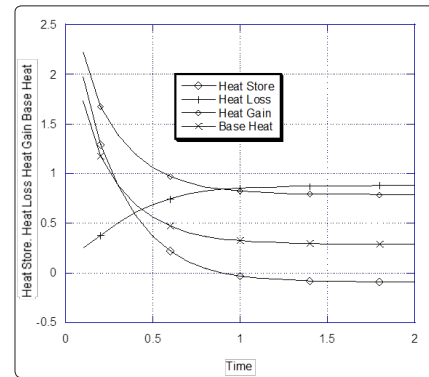


Figure 4c: Effect of heat generation parameter $Q_{gen}=1$ on heat profile

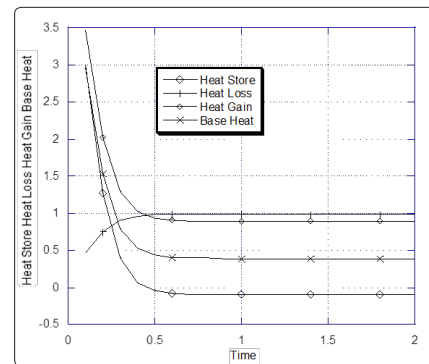


Figure 4d: Effect of heat generation parameter $Q_{gen}=3.0$ on heat profile

Conclusion

In the work reported herein we have studied the transient heat and temperature response to changes in certain fin parameters. The effects of the power law index, thermo-geometric, conduction, and heat generation parameters have been studied numerically. It was shown that they all play a very important role in the overall performance of the fin and can be used as very significant factors in fin design.

References

1. Campo A and Rodriguez F (1998) Approximate analytic temperature solution for uniform annular fins by adopting the power series method. Int. Jnl. Commun. Heat and Mass Trans 25: 809-818.
2. Arauzo I, Campo A and Cortez C (2005) Quick estimate of the heat transfer characteristics of annular fins of hyperbolic profile

- with power series method, *Appl. ThermEngr* 25: 623-634.
3. Yu LT and Chen CK (1998) Application of Taylor transformation to optimize rectangular fins with variable thermal parameters, *Appl. Math. Mod* 22: 11-21.
 4. AgwuNnanna AG, Haji-Sheik A, and Agonafer D (2003) Effect of variable heat transfer coefficient, fin geometry and curvature on the thermal performance of extended surfaces, *ASME J. Heat Transf* 456-460.
 5. Chiu CH and Chen CK (2002) A decomposition method for solving convective longitudinal fins with variable thermal conductivity 25: 2067-2975.
 6. Bahadur R and Bar-Cohen (2007) A. Orthotropic thermal conductivity effect on cylindrical pin fin heat transfer, *Int. Jnl. Heat Mass Transf* 115-1162.
 7. Aziz A and Rahman MM (2009) Thermal performance of a functionally graded radial fin, *Int. Jnl. Thermophysics* 1637-1648.
 8. Lewis R.W, Nithiarasu P and Seetharamu KN (2004) *Fundamentals of the Finite Element Method for heat and Fluid Flow*, John Wiley and Sons.
 9. Tannehill JC, Anderson DA and Pletcher RH (1997) *Computational Fluid mechanics and Heat Transfer*, 2nd ed. Taylor and Francis, Washington, D.C.
 10. Moitsheki RJ, Hayat T and Malik TY (2010) Some exact solutions of the fin problem with a power law temperature-dependent thermal conductivity, *Nonlinear Analysis, Real World Applications* 11: 3287-3294.
 11. Mhlongo MD and Moitsheki RJ (2014) Some exact solutions of nonlinear fin problem for steady heat transfer in longitudinal fin with different profiles, *Adv. Math. Physics* 1-16.
 12. Chapman AJ (1959) Transient heat conduction in annular fins of uniform thickness, *Ser* 55: 195-201.
 13. Donaldson AB and Shouman AR (1972) Unsteady temperature distribution in a convecting fin of constant area, *Appl. Sci. Res* 26: 75-85.
 14. Aziz A and Kraus AD (1995) Transient heat transfer in extended surfaces, *ASME Appld. Mech. Rev* 48: 317-350.
 15. Suryanarayana NV (1975) Transient response of straight fins *ASME Jnl. Heat Transf* 97: 417-423.
 16. Mao J and Rooke S (1994) Transient analysis of extended surfaces with convective tip, *Int. Comm. Heat and Mass Transfer* 21: 85-94.
 17. Mosayebidorcheh S, Farzinpoor M, and Ganji DD (2014) Transient thermal analysis of longitudinal fins with internal heat generation considering temperature-dependent properties and different fin profiles, *Energy Conv. Manage* 86: 365-370.
 18. Onur N (1996) A simplified approach to the transient conduction in a two-dimensional fin, *Int. Comm. Heat Mass* 23: 225-238.
 19. Aziz A and Torabi M (2012) Convective-radiative fins with simultaneous variation of thermal conductivity, heat transfer coefficient and surface emissivity with temperature, *Heat Trans-Asian Research* 41: 99-113.
 20. Campo A (1976) Variational techniques applied to radiative-convective fins with steady and unsteady conditions, *Warme-und Stoffubertragung* 9: 139-144.
 21. Moitsheki RJ and Harley C (2011) Transient heat transfer in longitudinal fins of various profiles with temperature-dependent thermal conductivity and heat transfer coefficient, *PranamaJnl. Physics* 77: 519-532.
 22. Moitsheki RJ (2008) Transient heat diffusion with temperature-dependent conductivity and time-dependent heat transfer coefficient, *Math. Problems Engrn*, Article ID 347568, doi:10.1155/2008/347568
 23. Campo A (1980) Comparison of three algorithms for nonlinear heat conduction problems, *Computers and Chem. Engrn* 4: 139-141.
 24. Campo A, Salazar A (1996) Similarity between unsteady- state conduction in a planar slab for short times and steady- state conduction in a uniform straight fin, *Heat and Mass Transf* 31: 365-370.
 25. Mahlekzadeh P, Rahideh H and Karami G (2006) A differential quadrature element method for nonlinear transient heat transfer analysis of extended surfaces, *Nu. Heat Transf* 49: 511-523.
 26. Sobamowo MG (2016) Thermal analysis of longitudinal fin with temperature-dependent properties and internal heat generation using Galerkin method of weighted residual, *Appld. Ther. Engrn* 99: 1316-1330.
 27. Sobamowo MG, Kamiyo OA and Adeleye OA (2017) Thermal performance analysis of a natural convection porous fin with temperature-dependent thermal conductivity and internal heat generation, *Ther. Sci. Engrn. Progress* 1: 39-52.
 28. Sutradhar A and Paulinio GC (2004) The simple boundary element method for transient heat conduction in functionally graded materials, *Coput. Mthds. Appld. Mech. Engrn* 193: 4511-4539.
 29. Bialecki R, Khun G (1993) Boundary element solution of heat conduction in problems in multizone bodies of nonlinear materials, *Int. Jnl. Num. Mthds* 36: 799-809.
 30. Sutradhar A, Paulino GH and Gray LJ (2002) Transient heat conduction in homogeneous and nonhomogeneous materials by the Laplace transform Galerkin boundary element method, *Engrn. Analysis Bound. Elem. Mthd* 26: 119-132.
 31. Onyejekwe OO (2016) Localized boundary-domain integro-partial differential formulations for transient scalar transport problems, *Int. JnlAppld. Comput. Math.* doi: 10.1007/s40819-016-0235.

Copyright: ©2019 Uchida Keitaroh. This is an open-access article distributed under the terms of the Creative Commons Attribution License, which permits unrestricted use, distribution, and reproduction in any medium, provided the original author and source are credited.